African Journal of Advanced Pure and Applied Sciences (AJAPAS)
*Online ISSN: 2957-644X*
Volume 4, Issue 4, 2025
Page No: 01-12
Website: https://aaasjournals.com/index.php/ajapas/index
ISI 2025: 1.126 SJIFactor 2024: 6.752 معامل التأثير العربي: 1.62

# Searching for the Optimum Operating Conditions for Methanol Synthesis Reactor Separator Loop by Using Genetic Algorithms

Saleem Fathi Almasalati [*1], Dr. Ali Elhudhiry [2], Shams Khaled [3]
[1,2,3] Chemical Engineering Department, Faculty of Engineering, University of Benghazi, Libya

# البحث عن طريق التشغيل المثالية لمنظومة المفاعل والفاصل لإنتاج الميثانول باستخدام الخورزميات الجينية

سليم فتحي [*1]، د. على حامد [2]، شمس خالد [3]
[3،2،1] قسم الهندسة الكيميائية، كلية الهندسة، جامعة بنغازي، ليبيا

[*]Corresponding author: salimeoeoeo@gmail.com

| Received: July 30, 2025 | Accepted: September 19, 2025 | Published: October 06, 2025 |
|---|---|---|

**Abstract:**
With the growing importance of methanol in the fuel industry, there is a pressing need to develop advanced models to optimize its production. In this thesis, a typical methanol production plant was modeled. The model was numerically solved using MATLAB and validated with published data. Next, genetic algorithms was used to seek the optimum operating conditions including feed temperature, feed pressure, and cooling temperature (shell temperature). The model showed a very good agreement with published data. Moreover, the current results were in excellent agreement when compared to the results of ASPEN-PLUS for the same plant. The optimization results showed a significant improvement in methanol production where the production rate increased by 71.35%. The production rate reached 13.0537 kg/s at conditions of T shell = 200 C, T = 205 C and P = 50 x106 Pa. This was a substantial improvement compared to the baseline production rate of 7.6181 kg/s at *T*shell= 238 C, T = 250 C and P = 52 x 106 Pa.

**Keywords**: Methanol , MATLAB, ASPEN-PLUS**.**

**الملخص**
في ظل الأهمية المتزايدة للميثانول في صناعة الوقود، تبرز الحاجة إلى تطوير نماذج متقدمة لتحسين إنتاجه.
تستعرض هذه الأطروحة نموذجًا رياضيًا لمحطة إنتاج ميثانول نموذجية، تم حله عدديًا باستخدام MATLAB والتحقق من صحته مقارنة بالبيانات المنشورة. بالإضافة إلى ذلك، تم مقارنة النموذج الحالي بنموذج هجين موجود في الأدبيات. تم استخدام الخوارزميات الجينية للبحث عن ظروف التشغيل المثلى، بما في ذلك درجة حرارة التغذية، وضغط التغذية، ودرجة حرارة التبريد (درجة حرارة القشرة). علاوة على ذلك، تم دراسة تأثير نشاط المحفز على إنتاج الميثانول. أظهرت النتائج توافقًا جيدًا مع البيانات المنشورة، حيث أظهرت مقارنة مع نموذج هجين في الأدبيات توافقًا ممتازًا . عند استخدام الخوارزميات الجينية، تم تحسين ظروف التشغيل، مما أدى إلى زيادة كبيرة في معدل الإنتاج بنسبة 71.35%. حيث وصل معدل الإنتاج إلى 13.0537 كجم/ثانية عند ظروف تشغيلية محددة، مقارنة بمعدل الإنتاج الأساسي البالغ 7.6181 كجم/ثانية.
تُظهر هذه الدراسة أهمية استخدام النماذج الرياضية المتقدمة وخوارزميات التحسين في تحسين عمليات الإنتاج الصناعي، مما يسهم في زيادة الكفاءة وتقليل التكاليف.

**الكلمات المفتاحية:** ميثانول ، MATLAB ، ASPEN-PLUS.

## I. Introduction

Methanol is one of the most important chemicals in the chemical industry. It's primarily used as an intermediate for producing formaldehyde, amines, and acetic acid, and also as a solvent. The development of the fuel industry has significantly increased the importance of methanol in the market. It serves as a raw material for the production of fuel additives (methyl-tert-butyl ether) and the synthesis of dimethyl ether (Olah, et al., 2009).
The feedstock for the process is synthesis gas (syngas), a mixture of CO2, CO, and H2.

Methanol production is affected by a number of operating factors including feed temperature, feed pressure, feed composition, cooling temperature (shell temperature), and recycle ratio. Consequently, most of the published optimization solutions centered on the indicated parameters.

Many investigations on methanol process optimization have been recorded; most concentrate on the urgitype reactor as the potential candidate for improvement. (Lovik, 2001) said a modeling, estimation, and optimization of a Lurgi shell and tube methanol synthesis reactor utilizing both pseudo homogeneous and heterogeneous mathematical models were researched. (Shahrokhi and Baghmisheh, (2005) studied modeling, optimization, and control of a Lurgitype reactor aiming to maximise reactor yield by altering shell temperature, feed composition, and recycle. ratio. An optimization study carried out by Fuad et al., 2012 took catalyst deactivation into account. They incorporated coolant temperature, inlet temperature and composition, feed flowrate, decision variables to maximize methanol production rate. (Kordnejad et al., 2013) presented a real time optimization (RTO) of an industrial shell and tube methanol reactor. The goal of their study was to maximize methanol production. Genetic algorithm was used to find out the best set of variables such as coolant feed flowrate and shell-side temperature.

(Stoica et al., 2015) investigated optimizing a gas-phase methanol reactor for maximizing carbon oxide conversion and methanol production. Formulating an optimization problem relevant to both direct and indirect cooling arrangements, they solved the reaction system's natural equilibrium limits.

(Bukhtiyarova Studied the impact of benzene presence in the feed stream and verified ideal conditions for effective methanol generation (et al., 2017). The aim of their work was to find optimal conditions to obtain a high efficiency of methanol production and low concentrations of side products. (Keshavar et al., 2020) has investigated a novel in which a novel configuration (NC), the gas-cooled reactor is modified and consists of three sections including shell, tubes, and mesh. (Samimi et al., 2020) employed a numerical model for a typical methanol synthesis plant for CO2 conversion. Their study focused on the effect of inert gases on methanol production.

## II. Methanol synthesis process

Popular in the 1960s, low-pressure methanol synthesis techniques usually running between 50 and 110 bar—took over from the prior high-pressure approach using a Cr-based catalyst.

Usually created as a shell and tube heat exchanger, a classic boiling-water methanol reactor packs the catalyst (often $CuO/ZnO/Al_2O_3$ ) in vertical tubes surrounded by In the shell, boiling water regulates the reactor temperature by means of pressure.

Equilibrium of the mechanisms in progress limits methanol conversion; in a high pressure separator, the reactor effluent is cooled to a low temperature to obtain liquid crude methanol product. The separator's recycled vapor is compressed to the reactor pressure. A little purge prevents inert gases from gathering in the loop.

Stream is used. The process flow diagram for the synthesis loop appears in Figure 1.

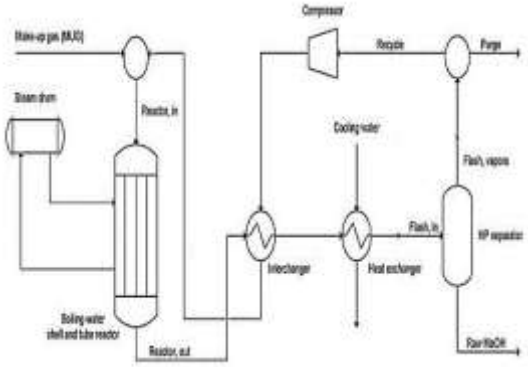


**Figure 1:** Methanol synthesis loop.

The important reactions taking place in a typical methanol reactor are the hydrogenation of CO and CO, and the reverse water-gas shift reaction.

$$CO + 2H_2 \leftrightarrow CH_3OH, \qquad \Delta H_{298} = -90.55 \frac{kJ}{mol} \tag{1}$$

$$CO_2 + 3H_2 \leftrightarrow CH_3OH + H_2O, \qquad \Delta H_{298} = -49.33 \frac{kJ}{mol} \tag{2}$$

$$CO_2 + H_2 \leftrightarrow CO + H_2O, \qquad \Delta H_{298} = 41.12 \frac{kJ}{mol} \tag{3}$$

The three reactions are not independent, and any one of them can be expressed as a linear combination of the other two.

**III. Modelling of methanol synthesis process** A homogenous (gas-phase) steady state model of the reactor is formulated here based on mass and energy balances. For the separator, the vapor pressure as a function of temperature was based on Soave-Redlich-Kwong equation of state. The vapor phase is partially recycled to the reactor.

**Reactor model**

Earlier I noted that Eq. (1)–(3) represent the processes occurring inside the reactor. The heat generated by the reaction is eliminated by circulating the shell-side cooling eater. Eq. (4) and (5) provide a group of basic ordinary differential equations (ODEs) that describe mass and energy balances throughout the catalytic reactor.

$$\frac{dy_i}{dz} = \frac{r_i \rho_B A_C \eta_i a}{F_t} \quad (4)$$

$$\frac{dT}{dZ} = \frac{\pi D_i}{F_t C_P} U_{shell} (T_{shell} - T) + \frac{\rho_B a A_C}{F_t C_P} \sum_{i=1}^{N} \eta_i r_i (-\Delta H_{f,i}) \quad (5)$$

**Table 1:** MUG variables in the process.

| Parameters | Value | Units |
|---|---|---|
| **Total flow rate** | 4685 | Ibmol/h |
| **Pressure** | 750 | Psi |
| **Temperature** | 250 | $^{o}$C |
| **Compositions** | | |
| **[$CH_3OH$]** | 0 | Mol.fr. |
| **[$CO_2$]** | 0.032 | Mol.fr. |
| **[CO]** | 0.285 | Mol.fr. |
| **[$H_2O$]** | 0 | Mol.fr. |
| **[$H_2$]** | 0.675 | Mol.fr. |
| **[$CH_4$]** | 0.006 | Mol.fr. |
| **[$N_2$]** | 0.003 | Mol.fr. |

**Table 2:** List of parameters.

| Parameters | Value | Units |
|---|---|---|
| **Length of reactor** | 7 | M |
| **Number of tubes** | 6560 | - |
| **Heat transfer coefficient** | 631 | W/($m^2$k) |
| **Catalyst bulk density** | 1100 | Kg/$m^3$ |
| **Catalyst activity** | 1 | - |
| **Internal dimeter of tubes** | 1.3 | In. |
| **Void fraction** | 0.38 | |
| **Shell temperature** | 238 | $^{0}$C |
| **Flash Pressure** | 730 | Psi |
| **Flash Temperature** | 65 | $^{0}$C |
| **Ratio of purge to vapor flow from flash** | 0.01 | |

**Kinetics**

As described by (Bussche and Froment, 1996) the Kinetics are based just reaction (1) and (3) in contrast to that of (Graaf et al.,1990). which is derived from all three reactions. (Graaf et al.,

1990) failed to explain, though, that some intermediates like the formyl and methoxy species are anticipated simultaneously in their feature in two simultaneous separate reactions.

According to the Langmuir–Hinshelwood–Hougen–Watson (LHHW) mechanism, the kinetics of methanol production are determined by a redox mechanism for the reverse water gas shift reaction. Via format, the hydrogenation reaction. The experimental setup for the founding kinetic model's development was as follows:

Temperature: 180–280 $^0$C; Pressure: 15–51 bar; Catalyst: ICI 51–2 $Cu/ZnO/Al_2O_3$ Constants for Bussche and Froment (1996) kinetic model are listed in Table 3.

**Table 3**: Kinetic Model Constants for Methanol Synthesis Reactions (Bussche and Froment, 1996).

| $K = Aexp(^{B}/_{RT})$ | A | B |
|---|---|---|
| $k_{MeOH}$ | 1.07 | 36,696 |
| $k_{RWGS}$ | 1.22 x $10^{10}$ | -94,765 |
| $k_1$ | 3453.38 | - |
| $k_2$ | 0.499 | 17,197 |
| $k_3$ | 6.62 x $10^{-11}$ | 124,119 |

**Table 4:** Reaction equilibrium constants.

| $K_{eq} = 10^{(^{A}/_{T-B})}$ | A | B |
|---|---|---|
| $K_{eq}^1$ | 3066 | 10.592 |
| $K_{eq}^2$ | -2073 | -2.029 |

The rate expressions for the two rate-determining steps are given below and the values of the rate constants and the equilibrium constants are given in Tables 3 and 4.

$$r_{MeOH} = \frac{K_{MeOH} p_{CO_2} p_{H_2} \left[1 - (\frac{1}{K_{eq}^1})(p_{H_2O} p_{CH_3OH} / p^3_{H_2} p_{CO_2})\right]}{(1 + K_1 \left(\frac{p_{H_2O}}{p_{H_2}}\right) + K_2 \sqrt{p_{H_2}} + K_3 p_{H_2O})^3} \quad (6)$$

$$r_{RWGS} = \frac{K_{RWGS} p_{CO_2} \left[1 - K_{eq}^2 (p_{H_2O} p_{CO} / p_{CO_2} p_{H_2})\right]}{(1 + K_1 \left(\frac{p_{H_2O}}{p_{H_2}}\right) + K_2 \sqrt{p_{H_2}} + K_3 p_{H_2O})} \quad (7)$$

**Separator model**

To forecast the nonideal behavior of polar compounds in the system, the flash separator shown in Fig. 1 has to be modeled (Chang, et al., 1986). pointed out that the components CO, H2, and CO2 display almost ideal behavior because the reaction temperature of 200–400 0C is far greater than their critical temperatures. Because of their polar molecular structure, $CH_3OH$ and $H_2O$ vapors are quite non ideal at these temperatures; that is, Vapor pressures must be estimated to determine the k-values, as ratio of saturated vapor pressure and total pressure, and hence the ideal vapor-liquid equilibrium composition. precisely guessed at the supplied temperature.

Due to the need for simplicity and accuracy in predicting k-values for a wide range of temperature, use of an equation of state (EOS) was considered. The form of the EOS is (Soave, 1972):

$$P = \frac{RT}{V_m + c - b} - \frac{a}{(V_m + c)(V_m + c + b)} \quad (8)$$

where $a = a_0 + a_1$ and the quadratic mixing term, a0 and the asymmetric polar term, a1 are given by

$$a_0 = \sum_{i=1}^{N} \sum_{j=1}^{N} y_i y_j \sqrt{a_i a_j} \, (1 - K_{ij}) \quad (9)$$

$$a_1 = \sum_{i=1}^{N} y_i \left( \sum_{j=1}^{N} y_j ((a_i a_j)^{\frac{1}{2}} \iota_{ji})^{1/3} \right)^3 \quad (10)$$

Where

$$b = \sum_{i=1}^{N} y_i b_i\,,\quad c = \sum_{i=1}^{N} y_i c_i\,,\quad a_i = f\left(T, T_{ci}\,,\quad P_{ci}\,,\, w_i\right), \tag{11}$$

$$b_i = f(T, T_{ci}, P_{ci}) \; and \; c_i = 0.40768 \left(\frac{RT_{ci}}{P_{ci}}\right)(0.29442 - z_i) \tag{12}$$

**Table 5 presents the** critical temperatures, pressures**,** and acentric factors from (Reid et al., 1997).

**Table 5:** Thermodynamic parameters for the components.

| Parameter | $CH_3OH$ | $CO_2$ | CO | $H_2O$ | $H_2$ | $CH_4$ | $N_2$ |
|---|---|---|---|---|---|---|---|
| $T_C$(k) | 512.6 | 304.1 | 132.9 | 647.3 | 33 | 190.4 | 126.2 |
| $P_C$(bar) | 80.9 | 73.8 | 35 | 221.2 | 12.9 | 46 | 33.9 |
| $w_i$ | 0.556 | 0.239 | 0.066 | 0.344 | -0.216 | 0.011 | 0.039 |

For a P–T flash the mass balance for each component is given by:

$$Fy_i = F_l l_i + F_v v_i \tag{13}$$

$$\sum_{i=1}^{N} l_i = 1 \tag{14}$$

$$\sum_{i=1}^{N} v_i = 1 \tag{15}$$

$$l_i \phi_{l,i} = v_i \phi_{v,i} \tag{16}$$

where **l and v represent the liquid and vapor output streams from** the flash and **yi are the mole fractions of component i in the feed to** the flash.
The **SRK EOS is used to compute** the **fugacity coefficients**. The k-value is the ratio:

$$K_i = \frac{v_i}{l_i} \tag{17}$$

**The Rachford–Rice equation provides** the fraction of vapors:

$$\sum_{i=1}^{N} \frac{y_i(K_i - 1)}{1 + \beta(K_i - 1)} = 0 \tag{18}$$

**Genetic Algorithms**

The Genetic algorithms (GAs) were first presented by (Holland, 1975) based on the mechanics of natural selection by Darwin and the natural genetics of Mendel. These algorithms are different from conventional optimization techniques; they perform random searches in a specified set of possible solutions in order to find the best solution based on quality or satisfaction criteria (Blasco, et al., 2001). In this work, the Genetic Algorithm is coded in MATLAB and compared its performance with Aspen Plus.

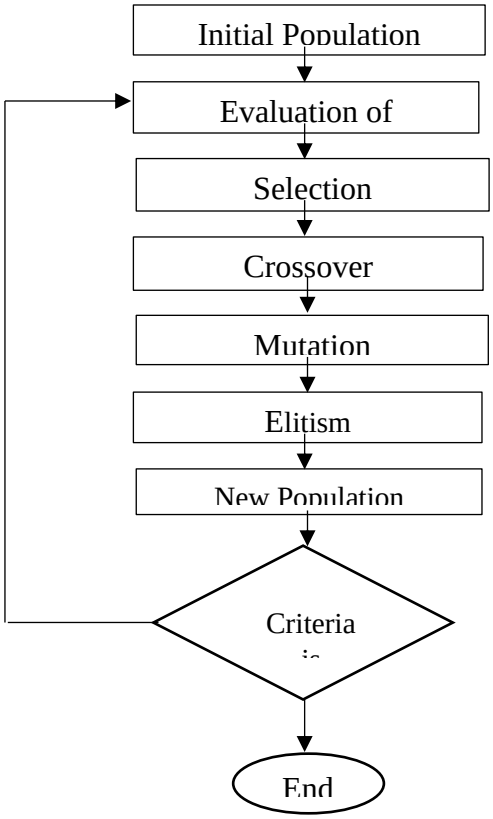


**Figure 2:** GA description flowchart

The first step in GAs is to create a random initial population. Because we are dealing with seven parameters, seven-bit chromosomes will be used in our populations. After that, the fitness function for each chromosome will be calculated and evaluated using equation (19). Stronger chromosomes will have a greater chance to be selected as parents in order to create new chromosomes which are called offsprings.

Offsprings which are produced through crossover and mutation operators inherit features from their parents so they can give better solutions (Haupt & Haupt, 2004). All the chromosomes including the initial populations and the offsprings will be collected in order to choose the best ones as new populations.

In the last step, the new population will be tested "If the criteria has been met end and this is the solution that we are looking for. Otherwise go to step two". The same steps will be repeated again and the process will be caried on until the best solution is obtained. The flowchart in Figure 2 demonstrates the GA description.

**Simulation Results and discussion**

This section presents the simulation results and discussion. The first part demonstrates the modelling results. Moreover, the second part shows the results after applying the genetic algorithms "optimization results".

**Modelling results**

The results of methanol model and simulation are presented in this part. The blue curve represents our simulation on Aspen Plus and the orange curve represents our model on MATLAB.

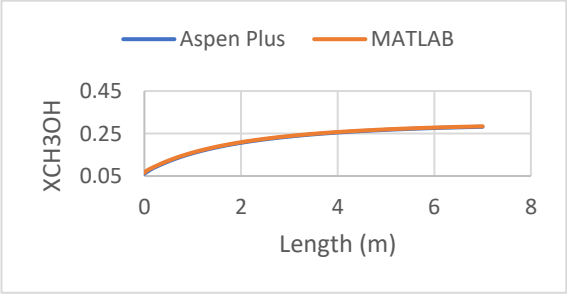


**Figure 3:** Composition of Hydrogen

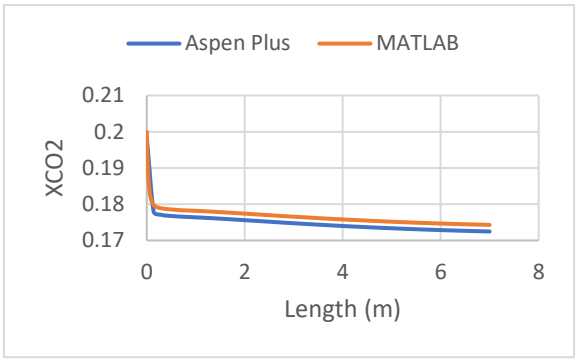


**Figure 4:** Composition of $CO_2$

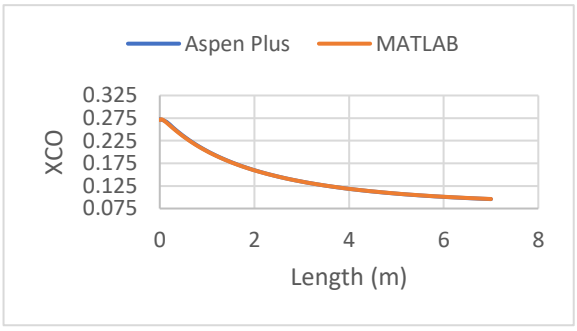


**Figure 5:** Composition of CO

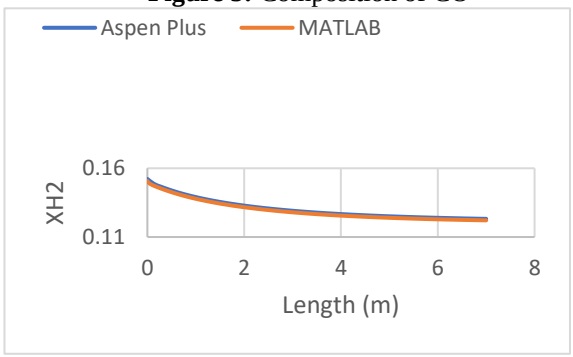


**Figure 6:** Composition of Methanol

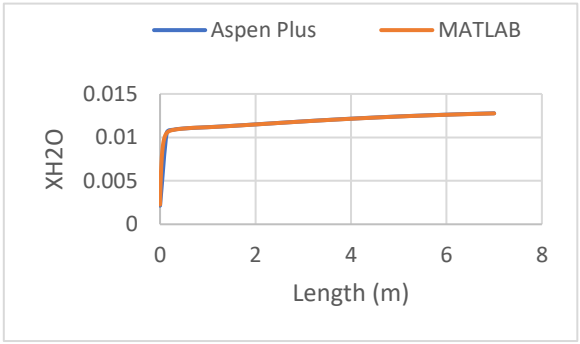


**Figure 7:** Composition of water

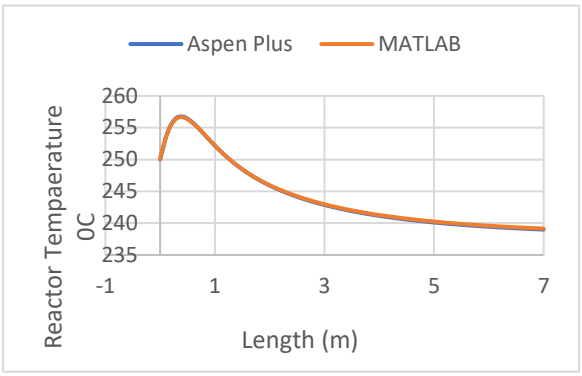


**Figure 8:** Reactor Temperature profile**.**

Simultaneous solutions of mass and energy balance for a one-dimension methanol reactor was presented in Figures 3 to 8. In Figure 3, a variation of H2 mass fraction against reactor distance was obtained with a very good agreement with the reactor simulation of published work (Abrol and Hilton, 2012).

Results of mass balance equation solution illustrated in Figure 4 shows a good matching between MATLB and Aspen Plus solutions in which mass fraction of CO2 against reactor length. Where a sudden sharp decrease in CO2 mass fraction due to the reaction. This sharp decrease in CO2 mass fraction ended near to the distance of less than 0.5 m. Beyond this distance, the sharp decrease in CO2 mass fraction started to be more regular with almost constant slope of CO2 mass fraction against reactor length.

The behavior in Figure 5 was different compared to CO2 curve. A smooth curve of CO mass fraction against reactor distance was obtained for Aspen Plus solution as well as MATLAB results.

Methanol mass fraction against reactor distance was shown in Figure 6. A positive proportionality relation is obtained till a distance of about 7 m. After that, the curve started to be aboriginal. In other hand, methanol composition started to be uniform.

Figure 7 shows a direct proportionality of water composition against reactor distance. A sudden increase of water mass fraction in a short reactor length as a mater of fact. This attitude is an opposite to the CO2 consumption presented in Figure 4.

The result of energy balance was presented in Figure 8 which shows a sharp of temperature peak at a distance of 0.5 m. This peak was naturally expected due to nature of the reaction behavior (exothermic). A uniform decrease of the temperature curve started at a distance of 4 to 5 m. Maximum temperature of about 257 C was obtained and the minimum temperature of about 239 C which were resulted within the working temperature.

**GA optimization**

In this work, the main task is to calculate the optimum parameters that maximize methanol production by using GA optimization technique. The first step is to encode the problem into suitable GA chromosomes and then construct the population. Real numbers rather than binary encoding is considered due to the tuning parameters are normally represented in real numbers. 20 chromosomes are selected for the population size in each generation. Each chromosome comprises of four parameters [Tshell, T, P,]. The fitness function is developed to minimize the production of MeOH as follows:

Maximize f1 = f (Tshell, T, P,) (19)

Subjected to:

Tupper < T < Tlower

Pupper < P < Plower

Tshellupper < Tshell < Tshelllower

Where:

f1 is the objective function of the methanol

T feed temperature

P feed pressure

Tshell cooling temperature .

The GA is coded in MATLAB file with respect to the setting parameters and the selected values that are shown in Table 6.

**Table 6**: Genetic Algorithm Settings and Optimization Parameters for Methanol Production.

| GA Property | Methods/Values | |
|---|---|---|
| Number of generations | 30 | |
| Population Size | 20 | |
| Number of variables $(n\,\mathrm{var})$ | 3 | |
| Number of objective functions | 1 | |
| Selection method | Tournament Selection | |
| Crossover method | SBX | |
| Probability of Crossover | 0.7 | |
| Distribution index in SBX | 20 | |
| Mutation method | Polynomial mutation | |
| Probability of Mutation | $1/(n\,\mathrm{var})$ | |
| Distribution index in polynomial mutation | 20 | |
| Lower bound vector of optimization variables | (Tshelllower, Tlower, Plower) | (200, 200, 4e+6) |
| Upper bound vector of optimization variables | (Tshelluppar, Tuppar, Puppar) | (250, 280, 5.2e+6) |

**Optimization results**

As the problem is developed as a single-objective optimization problem, this section shows the results after applying genetic algorithms. The results are presented in Figures 9 to 13.

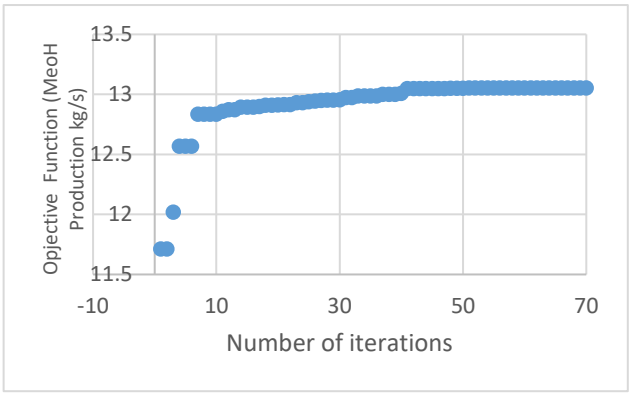


**Figure 9:** GA solutions**.**

Figure 9 illustrates methanol production against the number of numerical iterations been applied by GA. Which shows stable results to achieve the conversions**.**

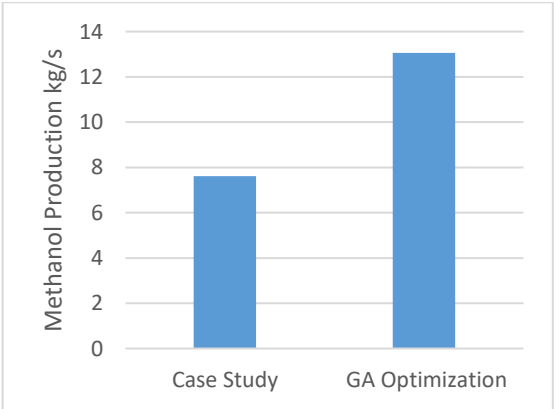


**Figure 10:** Methanol production before and after applying GA.

Figure 10 shows a comparison of MeOH production rate between a case study published by (Abrol and Hilton, 2012) and our case using GA. A higher production rate of 13.0537 kg/s was obtained at optimum operation conditions of Tshell= 200 C, T= 205 C and P= 4e+6 pa compared to a value of 7.6181 kg/s obtained at Tshell= 238 C, T= 250 C and P= 5.2e+6 pa.

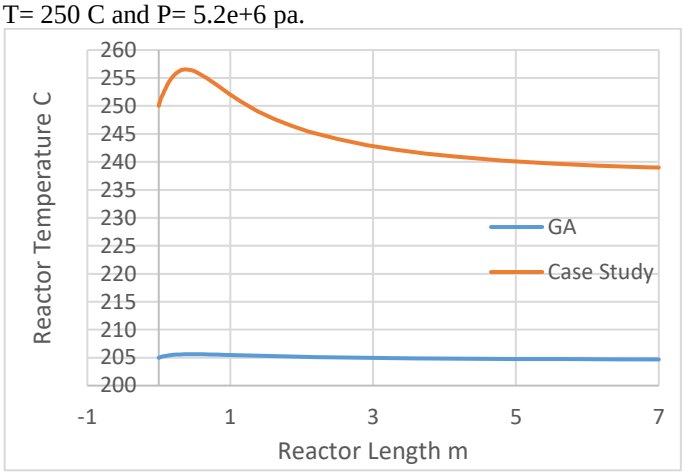


**Figure 11:** Temperature profile.

Figure 11 demonstrates the temperature profile of the reactor along with distance z. The orange curve illustrates the conventional behavior, showing high temperature peak at the beginning of the reactor zone and slowly comes down along with z till a temperature of less than 240 C. While by applying the GA which allows to calculate the optimum feed temperature of T= 205 C, a smooth profile was achieved and the range of the reactor temperature was trapped between 204.683 C to 205.613 C.

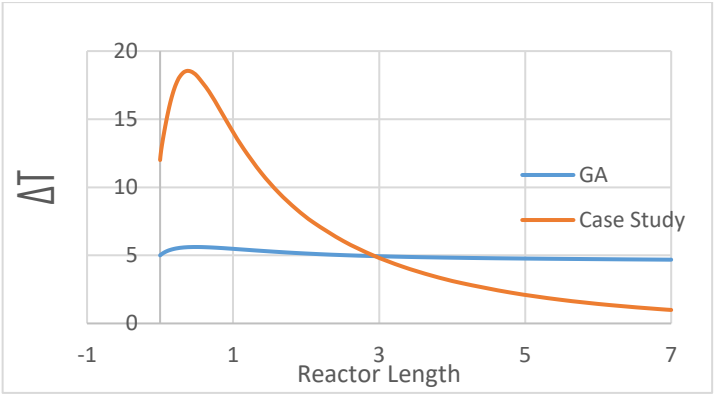


**Figure 12**: T – shell against reactor length.

Figure 12 shows the temperature difference between the catalyst tube temperature and the shell temperature (driving force) against the reactor distance. A temperature peak was found due to the exothermic effect of the reaction. This temperature peak will disappear along with the reactor distance.

By using GA, the optimum temperature of the feed stream and the cooling fluid stream were obtained. As it is shown in the blue curve in Figure 13, the temperature difference between the optimum shell and tube temperature allow to avoid the temperature peak as the shell and tube temperature became close to each other with maximum difference of 5.613 C. This will permit to approximate temperature difference with less error concerning the estimation of the physical properties of the mixture. Moreover, this will make the reactor energy balance closer to isothermal conditions and will become easier to deal with.

## CONCLUSION

In this study, a methanol process has been numerically modeled using MATLB. The process was simulated on Aspen Plus to confirm accuracy of our model. Optimum operating conditions including feed temperature, feed pressure and cooling temperature (shell temperature) were calculated by using genetic algorithms. The main goal of this work is to maximize methanol production by estimating the optimum operating conditions. The results show that after applying genetic algorithms, methanol production increased by 71.35% of production rate 13.0537 kg/s obtained at Tshell = 200 C, T = 205 C and P = 4e+6 pa compared to a value of 7.6181 kg/s obtained at Tshell= 238 C, T= 250 C and P= 5.2e+6 pa. The activity of the catalyst is one of the factors that depend on the working time.

**Nomenclature**

$\boldsymbol{a}$ activity of catalyst
$\boldsymbol{a_0}$ quadratic mixing term
$\boldsymbol{a_1}$ asymmetric polar term
$\boldsymbol{A_C}$ cross − sectional area of reactor tube
$\boldsymbol{C_P}$ specific heat at constant pressure
$\boldsymbol{D_i}$ internal diameter of reactor tube
$\boldsymbol{F_t}$ total molar flow rate
$\boldsymbol{k_i}$ kinetic factor for reaction i
$\boldsymbol{K_{ij}}$ binary interaction parameter for pair i and j
$\boldsymbol{K_{eq}^i}$ equilibrium constants for reaction i
$\iota_i$ composition of component i in liquid from flash
$\boldsymbol{N}$ number of components
$\boldsymbol{P}$ pressure
$\boldsymbol{P_i}$ partial pressure of component i
$\boldsymbol{r_i}$ rate of reaction for component i
$\boldsymbol{T}$ temperature
$\boldsymbol{T_{shell}}$ temperature of boiling water on the shell side
$\boldsymbol{U_{shell}}$ overall heat transfer coefficient from reactor tube side to shell − side
$\boldsymbol{\nu_i}$ $composition\ of\ component\ i\ in\ vapor\ from\ flash$
$\boldsymbol{y_i}$ mole fraction of component i
$\boldsymbol{z}$ axial direction
$\boldsymbol{\beta}$ equilibrium separation in flash
$\boldsymbol{\phi_{\iota,i}}$ fugacity coefficient of component i in liquid
$\boldsymbol{\phi_{v,i}}$ fugacity coefficient of component i in vapor
$-\Delta\boldsymbol{H_{f,i}}$ heat of formation of component i at operating temperature T
$\boldsymbol{\eta_i}$ catalyst effectiveness factor
$\boldsymbol{\rho_B}$ density of catalyst bed

**REFERENCES**


[1] Soave, G. (1972). Equilibrium constants for modified Redlich–Kwong equation-ofstate. Chemical Engineering Science, 27, 1196–1203.

[2] Holland. J. H. (1975). Adaptation in Natural and Artificial Systems. The University of Michigan Press, Ann Arbor, MI.

[3] Meyer, R. A. (1984). In Handbook of synfuels technology. McGraw Hill Higher.

[4] Chang, T., Rousseau, R. W., & Kiipatrick, P. K. (1986). Methanol synthesis reactions: Calculations of equilibrium conversions using equations of state. Industrial and Engineering Chemistry Process Design and Development, 25, 477–481.

[5] Graaf, G. H., Scholtens, H., Stamhuis, E. J., & Beenackers, A. A. C. M. (1990). Intraparticle diffusion limitations in low-pressure methanol synthesis. Chemical Engineering Science, 45(4), 773–783.

[6] Bussche, K. M. V., & Froment, G. F. (1996). A steady-state kinetic model for methanol synthesis and the water gas shift reaction on a commercial Cu/ZnO/Al2O3 catalyst. Journal of Catalysis. 161, 1–10.

[7] Reid, R. C., Prausnitz, J. M., & Poling, B. E. (1997). The properties of gases and liquids (4th ed.). McGraw Hill.

[8] Lovik I. (2001). Modelling, Estimation and Optimization of the Methanol Synthesis with Catalyst Deactivation. Doctoral thesis. Norwegian University of Science and Technology. 127p.

[9] Haupt, R. L., & Haupt, S. E. (2004). Practical genetic algorithms. (2, Ed.) John Wiley & Sons.

[10] Shahrokhi M. and Baghmisheh G. (2005). Modeling, simulation and control of a methanol synthesis fixed bed reactor. Chemical Engineering Science. vol. 60. pp. 4275-4286.

[11] Olah G.A., Goeppert A. and Prakash G.K.S. (2009). Beyond oil and gas: the methanol economy. Wiley-VCH.

[12] Abrol S. and Hilton C.M. (2012). Modeling, simulation and advanced control of methanol production from variable synthesis gas feed. Computers and Chemical Engineering. Vol. 40. pp.117-131.

[13] Fuad M.N, Hussain M.A, and Zakaria A. (2012). Optimization strategy for long-term catalyst deactivation in a fixed-bed reactor for methanol synthesis process. Computers & Chemical Engineering. Vol. 44. pp. 104-126.

[14] Kordnejad M., Shokroo E.J. and Shahcheraghi M. (2013). REAL TIME OPTIMIZATION OF SHELL AND TUBE METHANOL REACTOR USING EVOLUTIONARY AND GENETIC ALGORITHMS. Petroleum & Coal. Vol. 55. pp. 322-329.

[15] STOICA I., BANU I., BOBARNAC I. and BOZGA G. (2015). OPTIMIZATION OF A METHANOL SYNTHESIS REACTOR. vol. 77. pp. 1454-2331.

[16] Bukhtiyarova M., Lunkenbein T., Kähler K. and Schlögl R. (2017). Methanol Synthesis from Industrial CO2 Sources: A Contribution to Chemical Energy Conversion. CrossMark. Vol. 147. pp. 416–427.
[17] Keshavarz A., Mirvakili A., Chahibakhsh S., Shariati A.R. and Rahimpour M.R. (2020). Simultaneous methanol production and separation in the methanol synthesis reactor to increase methanol production. Elsevier.
[18] Samimi F., Feilizadeh M., Najibi S.B. and Rahimpour M.R. (2020). Carbon dioxide utilization in methanol synthesis plant: process modeling. Vol. 38.
[19] Wolday A.K., Gujarathi A.M and Ramteke M. (2023). Multi-objective optimization of methanol production for energy efficiency and environmental sustainability. Computers and Chemical Engineering. Vol. 179